Acta Crystallographica Section F
Structural Biology and Crystallization Communications
ISSN 1744-3091

Expression, purification and crystallization of an indole prenyltransferase from *Aspergillus fumigatus*

Jing Chen,[a,b] Hiroyuki Morita,[a] Ryohei Kato,[c] Hiroshi Noguchi,[b] Shigetoshi Sugio[c]* and Ikuro Abe[a]*

[a]Graduate School of Pharmaceutical Sciences, The University of Tokyo, 7-3-1 Hongo, Bunkyo-ku, Tokyo 113-0033, Japan, [b]School of Pharmaceutical Sciences and GCOE Program, University of Shizuoka, 52-1 Yada, Suruga-ku, Shizuoka 422-8526, Japan, and [c]Biotechnology Laboratory, Mitsubishi Chemical Group Science and Technology Research Center Inc., 1000 Kamoshida, Aoba-ku, Yokohama, Kanagawa 227-8502, Japan

Correspondence e-mail: sugio.shigetoshi@mw.m-kagaku.co.jp, abei@mol.f.u-tokyo.ac.jp

Received 21 December 2011
Accepted 4 February 2012

CdpNPT from *Aspergillus fumigatus* is a dimethylallyltryptophan synthase/indole prenyltransferase that catalyzes reverse prenylation at position N1 of tryptophan-containing cyclic dipeptides. Residues 38–440 of CdpNPT were expressed in *Escherichia coli* and crystallized using the sitting-drop vapour-diffusion and microseeding techniques. The crystals belonged to space group $P2_12_12_1$, with unit-cell parameters $a = 84.4$, $b = 157.1$, $c = 161.8$ Å, $\alpha = \beta = \gamma = 90.0^\circ$.

1. Introduction

The fungal indole prenyltransfereases (PTs; EC 2.5.1.1; dimethylallyltransferases) catalyze the prenylation of tryptophan and its derivatives with dimethylallyl diphosphate (DMAPP) as the prenyl donor in the biosynthesis of structurally diverse prenylated indole alkaloids including ergot alkaloids and terrequinone alkaloids (Steffan *et al.*, 2009; Li, 2009*a*,*b*). The enzymes show varying substrate specificities and regiospecificities for the prenylation of the indole core and the prenyltransfer reactions are classified into two types: 'regular' prenylation (attack at the primary centre of the dimethylallyl carbocation) and 'reverse' prenylation (attack at the tertiary centre). For example, FgaPT2 and FtmPT1 from *Aspergillus fumigatus* catalyze regular prenylation of L-tryptophan at position C4 and the indole nucleus of the cyclic dipeptide brevianamide F (cyclo-L-Trp-L-Pro) at position C2 (Fig. 1*a*) to produce the biosynthetic precursors of fumigaclavine C and fumitremorgin B, respectively (Steffan *et al.*, 2007; Unsöld & Li, 2005; Grundmann *et al.*, 2008). In contrast, CdpNPT from *A. fumigatus* Af293 catalyzes reverse prenylation at position N1 of L-tryptophan and tryptophan-containing cyclic dipeptides such as cyclo-L-Trp-L-Trp and cyclo-L-Trp-L-Tyr using DMAPP as the prenyl donor (Fig. 1*b*), although the physiological substrate and product of the enzyme reaction have yet to be elucidated (Zou *et al.*, 2009; Li, 2009*a*).

Although several indole PTs have previously been reported to exist as monomeric proteins (Cress *et al.*, 1981; Grundmann & Li, 2005; Steffan *et al.*, 2009), recent studies on the indole PT enzymes revealed that most of the enzymes form biologically active homo-

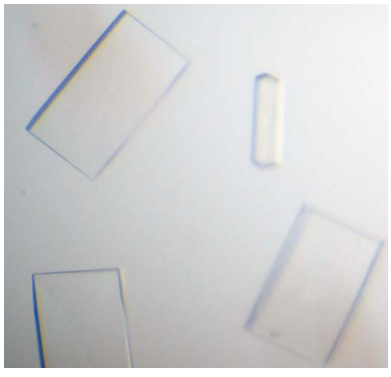

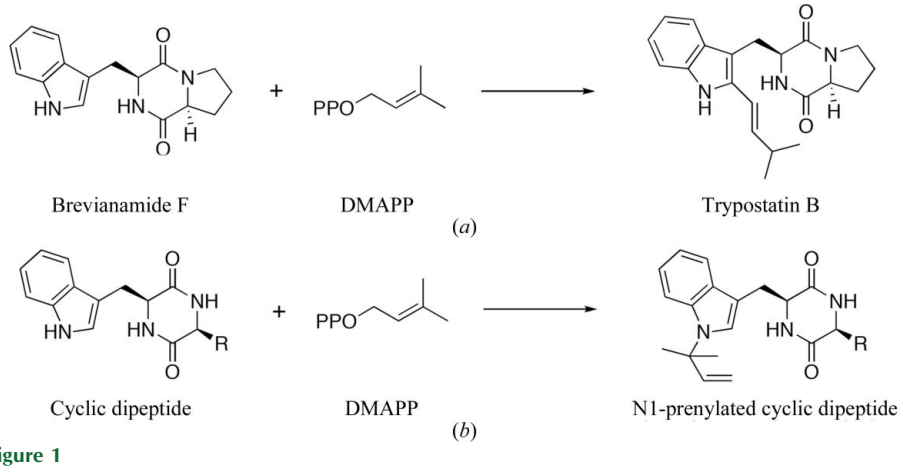

Figure 1
Prenyltransfer reactions catalyzed by FtmPT1 and CdpNPT. (*a*) Regular prenylation of brevianamide F at position C2 by *A. fumigatus* FtmPT1. (*b*) Reverse prenylation of the cyclic dipeptide at position N1 by *A. fumigatus* CdpNPT.

dimers composed of approximately 52 kDa subunits in solution (Metzger *et al.*, 2009; Jost *et al.*, 2010; Liu & Walsh, 2009; Steffan *et al.*, 2009). Furthermore, the X-ray crystal structures of *A. fumigatus* FgaPT2 and FtmPT1 revealed that the enzymes share the rare $(\alpha\alpha\beta\beta)_5$-barrel fold (Metzger *et al.*, 2009; Jost *et al.*, 2010), which was first observed in a bacterial aromatic PT enzyme, NphB, from *Streptomyces* sp. strain CL190 (Kuzuyama *et al.*, 2005). The structural analyses also suggested that modification of the active-site cavity results in alteration of the substrate specificities as well as the regiospecificities of the prenylation reactions. Notably, recent site-directed mutagenesis studies of FgaPT2 suggested that the enzyme initially catalyzes reverse prenylation and that a subsequent Cope rearrangement and re-aromatization reactions lead to the regular prenylation of L-tryptophan (Luk *et al.*, 2011).

CdpNPT (GenBank accession No. AFUA_8G00620), which catalyzes reverse prenylation at position N1 of tryptophan-containing cyclic dipeptides, was identified on chromosome 8 in *A. fumigatus* Af293 (Zou *et al.*, 2009; Li, 2009*a*). The enzyme is composed of 440 amino acids and shares 31 and 28% amino-acid sequence identity with *A. fumigatus* FgaPT2 and FtmPT1, respectively. A sequence comparison revealed that the dimethylallyl diphosphate-binding residues (Arg100, Tyr187, Tyr261, Lys259, Tyr345, Tyr409 and Tyr413) and the catalytic residue (Glu89) of FgaPT2 and FtmPT1 are well conserved in CdpNPT (the numbering is that of FgaPT2). In contrast, several active-site residues are uniquely altered in CdpNPT. For example, the catalytic Lys174 residue in the FgaPTs, which plays an important role in the Cope rearrangement and re-aromatization reactions (Luk *et al.*, 2011), is uniquely replaced by Val in CdpNPT. Furthermore, Thr102 and Arg244 in FgaPT2, corresponding to Gly102 and His244, respectively, in FtmPT1, which are thought to determine the substrate specificities of the enzyme reactions (Jost *et al.*, 2010), are uniquely replaced by Ala residues in CdpNPT. To further clarify the structure–function relationship of the indole PT enzymes and to understand the intimate structural details of the enzyme-catalyzed processes, we expressed a truncated (38–440) His_6-fused *A. fumigatus* CdpNPT in *Escherichia coli* and obtained a good-quality crystal of the recombinant enzyme.

2. Experimental

2.1. Construction of the expression plasmid

The gene encoding full-length CdpNPT was amplified from the cDNA library of *A. fumigatus* Af293 (Stratagene) using the forward primer 5′-ATTTAT**CATATG**GACGGTGAGATGACCGCTTCT-3′ and the reverse primer 5′-TTATAT**CTCGAG**TTCAGGCCAAAAG-TAATATATAGA-3′ (the *Nde*I and *Xho*I restriction sites are indicated in bold). The amplified 1323 bp DNA fragment was digested with *Nde*I and *Xho*I and was ligated into the *Nde*I and *Xho*I sites of pET22b(+) (Novagen) using a DNA-ligation kit (TaKaRa) for expression as a fusion protein with a His_6 tag at the C-terminus.

The pET22b(+) vector encoding full-length CdpNPT was used as the template to amplify the gene encoding residues 38–440 of CdpNPT by PCR using the forward primer 5′-GGAATTC**CATAT-G**ATAGCTTATCATACCCTCAC-3′ and the reverse primer 5′-TTA-TAT**CTCGAG**TTCAGGCCAAAAGTAATATA-3′ (the *Nde*I and *Xho*I restriction sites are indicated in bold). The amplified 1212 bp DNA fragment was digested with *Nde*I and *Xho*I and was cloned into the *Nde*I/*Xho*I sites of the pET22b(+) expression vector (Novagen) to express the CdpNPT (38–440) mutant enzyme with a His_6 tag at the C-terminus.

2.2. Expression and purification

After confirmation of their sequences, the pET-22b(+) vectors encoding the full-length CdpNPT and the truncated CdpNPT (38–440) enzymes were independently transformed into *E. coli* BL21 (DE3) pLysS. The cells harbouring each plasmid were cultured to an OD_{600} of 0.6 in LB medium containing 100 µg ml^{-1} ampicillin at 303 K. Isopropyl β-D-1-thiogalactopyranoside was then added to a final concentration of 1 m*M* to induce gene expression and the cultures were incubated for a further 16 h at 303 K.

All of the following procedures were performed at 277 K for both the full-length and the truncated CdpNPTs. The *E. coli* cells were harvested by centrifugation at 5000*g* and resuspended in 50 m*M* Tris–HCl buffer pH 8.0 containing 0.1 *M* NaCl and 5%(*v*/*v*) glycerol (buffer *A*). The cells were disrupted by sonication six times for 10 s each with 15 s intervals between each sonication and the lysate was centrifuged at 12 000*g* for 30 min. The supernatant thus obtained was loaded onto an Ni Sepharose 6 Fast Flow column (GE Healthcare) equilibrated with buffer *A*. After washing the column with 50 m*M* Tris–HCl buffer pH 7.5 containing 200 m*M* NaCl and 5%(*v*/*v*) glycerol (buffer *B*), the His_6-tagged CdpNPT was subsequently eluted with buffer *B* containing 500 m*M* imidazole. The protein solution was then diluted fivefold with 50 m*M* Tris–HCl buffer pH 7.5 containing 5%(*v*/*v*) glycerol and 2 m*M* DTT (buffer *C*) and applied onto a Resource-Q column (GE Healthcare). The column was washed with buffer *C* containing 100 m*M* NaCl and the protein was subsequently eluted at 160 m*M* NaCl using a linear gradient of 100–500 m*M* NaCl. The protein solution was further purified to homogeneity by gel-filtration chromatography on Superdex 200 HR (10/300 GL; GE Healthcare) and was concentrated to 10 mg ml^{-1} in 20 m*M* Tris–HCl pH 7.5 containing 100 m*M* NaCl and 2 m*M* DTT. Dynamic light-scattering (DLS) analysis was performed using a DynaPro MSXTC molecular-sizing instrument (Protein Solutions Inc.). After centrifugation using a 0.22 µm Ultrafree-MC filter (Millipore) to remove particulate material from the protein solution, the solution properties of the purified protein were monitored. Data were acquired from 50 scattering measurements at 278 K; a total of three sets of data were analyzed using the *DYNAMICS* software package (Protein Solutions Inc.) and were averaged.

2.3. Crystallization and X-ray data collection

Initial crystallization attempts were performed at 278 and 293 K using the sitting-drop vapour-diffusion method by mixing 0.8 µl of either the purified full-length CdpNPT solution or the truncated His_6-tagged CdpNPT (38–440) solution with an equal volume of reservoir solution (using Wizard I and II from Emerald BioSystems and Crystal Screen and Crystal Screen II from Hampton Research) and equilibrating the mixture against 100 µl reservoir solution. Clusters of crystals were observed a week later using a crystallization solution consisting of 100 m*M* Tris–HCl pH 8.5, 200 m*M* lithium sulfate, 1.26 *M* ammonium sulfate. Further crystallization was attempted at various pH values, together with the use of 1.0–2.0 *M* ammonium sulfate, 200 m*M* lithium sulfate as precipitant, but diffraction-quality crystals were not obtained. Therefore, further optimization of the crystallization conditions was performed using the microseeding technique. The crystal clusters in the drop were crushed with a needle to produce a stock mixture of crystal seeds, which was then diluted 10^3-fold, 10^4-fold, 10^5-fold, 10^6-fold and 10^7-fold with reservoir solutions at various pH values, together with the use of 1.0–2.0 *M* ammonium sulfate, 200 m*M* lithium sulfate, 2 m*M* L-tryptophan as precipitant. An aliquot of 0.8 µl of each seed solution was subsequently mixed with an equal volume of the purified enzyme solution

and was again screened against the reservoir solutions. Diffraction-quality crystals were finally obtained using the His_6-tagged CdpNPT (38–440) enzyme solution at 293 K in 100 m*M* MES pH 6.5 containing 1.1 *M* ammonium sulfate, 150 m*M* lithium sulfate and 2 m*M* L-tryptophan using the sitting-drop vapour-diffusion method and the seeding technique.

The crystals were transferred into a cryoprotectant consisting of 100 m*M* MES pH 6.5, 1.1 *M* ammonium sulfate, 150 m*M* lithium sulfate, 2 m*M* L-tryptophan, 20%(*v*/*v*) glycerol. After a few seconds, the crystals were picked up in a nylon loop and flash-cooled at 100 K in a nitrogen-gas stream. X-ray diffraction data sets were collected from a single crystal on beamline X06DA at the Swiss Light Source using a MAR 225 CCD detector with a crystal-to-detector distance of 210 mm. The wavelength of the synchrotron radiation was 1.0000 Å. A total of 200 frames were recorded with a 0.5° oscillation angle and a 1 s exposure time. The data were indexed, integrated and scaled using the *HKL*-2000 program package (Otwinowski & Minor, 1997).

3. Results and discussion

Our initial crystallization trials using the full-length His_6-tagged CdpNPT did not yield any diffraction-quality crystals. This may be attributed to the high flexibility of the 37 N-terminal amino-acid residues, as predicted by a *DNASTAR* protein-chain flexibility search using the Karplus–Schulz method (flexibility threshold value = 1.0; Burland, 2000). Therefore, it was anticipated that truncation of the N-terminal amino-acid residues of CdpNPT would facilitate the generation of better diffracting crystals. The truncated His_6-tagged CdpNPT (38–440) was thus constructed and expressed in *E. coli*. The truncated enzyme exhibited identical prenylation activity for L-tryptophan to that of the full-length enzyme (data not shown). The typical yield was about 10 mg per litre of culture. The truncated His_6-tagged CdpNPT (38–440) migrated as a single band with a molecular mass of 47 kDa on SDS–PAGE, which agrees well with the calculated value of 46.7 kDa. In contrast, the recombinant enzyme yielded a molecular mass of 96 kDa in a gel-filtration experiment. Furthermore, DLS analysis after gel filtration revealed a monomodal distribution with a polydispersity value of 22.8% and an estimated molecular mass of 82 kDa, suggesting that the truncated His_6-tagged CdpNPT (38–440) also forms a homodimer, as in the case of the full-length CdpNPT. In contrast, truncation of the N-terminal 43 residues of CpaD, another fungal indole PT from *Aspergillus* sp., reportedly resulted in disruption of both the dimerization and catalytic activity (Liu & Walsh, 2009).

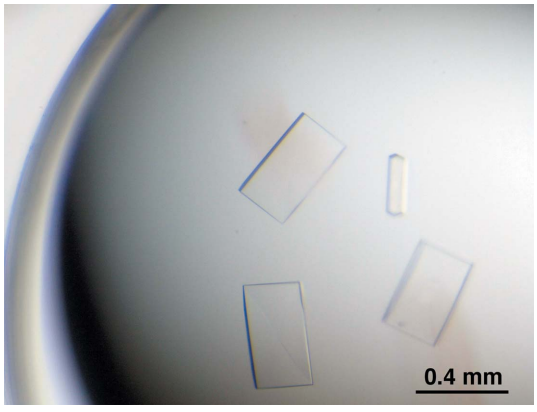

Figure 2
Crystals of the truncated His_6-tagged recombinant CdpNPT (38–440). The dimensions of the crystals are approximately 0.45 × 0.25 × 0.08 mm.

Table 1
Data-collection statistics.

Values in parentheses are for the highest resolution shell.

Beamline	X06DA, Swiss Light Source
Wavelength (Å)	1.00000
Temperature (K)	100
Detector	MAR 225 CCD
Crystal-to-detector distance (mm)	210
Oscillation angle (°)	0.5
No. of frames	200
Exposure time (s)	1
No. of crystals	1
Space group	$P2_12_12_1$
Unit-cell parameters	
a (Å)	84.4
b (Å)	157.1
c (Å)	161.8
$\alpha = \beta = \gamma$ (°)	90
Resolution (Å)	50.0–2.5 (2.59–2.50)
Total reflections	309778
Unique reflections	75494
Mosaicity (°)	0.27
Multiplicity	4.1 (3.8)
Completeness (%)	99.6 (96.8)
$\langle I/\sigma(I)\rangle$	23.8 (3.3)
R_{merge}† (%)	6.0 (31.9)

† $R_{merge} = \sum_{hkl}\sum_i |I_i(hkl) - \langle I(hkl)\rangle| / \sum_{hkl}\sum_i I_i(hkl)$, where $I(hkl)$ is the intensity of reflection hkl, $\sum_{hkl}$ is the sum over all reflections and $\sum_i$ is the sum over i measurements of reflection hkl.

Crystals appeared reproducibly within a week and the largest crystal grew to dimensions of approximately 0.45 × 0.25 × 0.08 mm (Fig. 2). A complete data set was collected to 2.5 Å resolution. Detailed data-processing statistics are shown in Table 1. Based on the diffraction data, the space group was determined to be $P2_12_12_1$, with unit-cell parameters $a = 84.4$, $b = 157.1$, $c = 161.8$ Å, $\alpha = \beta = \gamma = 90.0°$. With four monomers in the asymmetric unit, the Matthews volume (V_M; Matthews, 1968) was calculated to be 2.9 $Å^3\ Da^{-1}$ and the estimated solvent content was 56.5%, which is in the range normally observed for protein crystals. Structure determination using the molecular-replacement method with the *MOLREP* program (Vagin & Teplyakov, 2010) and a CdpNPT (38–440) structure model generated by the *SWISS-MODEL* package (http://expasy.ch/spdpv/) based on the crystal structure of *A. fumigatus* FgaPT2 (PDB entry 3i4x; Metzger *et al.*, 2009) as a search model is now in progress. Simultaneously, we are also attempting to crystallize the truncated His_6-tagged CdpNPT (38–440) complexed with substrate analogues. These structural analyses will provide valuable insights into the catalytic mechanism of the indole PT enzymes.

This work was supported in part by a Grant-in-Aid for Scientific Research from the Ministry of Education, Culture, Sports, Science and Technology, Japan.

References

Burland, T. G. (2000). *Methods Mol. Biol.* **132**, 71–91.
Cress, W. A., Chayet, L. T. & Rilling, H. C. (1981). *J. Biol. Chem.* **256**, 10917–10923.
Grundmann, A., Kuznetsova, T., Afiyatullov, S. S. & Li, S.-M. (2008). *Chembiochem*, **9**, 2059–2063.
Grundmann, A. & Li, S.-M. (2005). *Microbiology*, **151**, 2199–2207.
Jost, M., Zocher, G., Tarcz, S., Matuschek, M., Xie, X., Li, S.-M. & Stehle, T. (2010). *J. Am. Chem. Soc.* **132**, 17849–17858.
Kuzuyama, T., Noel, J. P. & Richard, S. B. (2005). *Nature (London)*, **435**, 983–987.
Li, S.-M. (2009*a*). *Phytochemistry*, **70**, 1746–1757.

Li, S.-M. (2009*b*). *Appl. Microbiol. Biotechnol.* **84**, 631–639.
Liu, X. & Walsh, C. T. (2009). *Biochemistry*, **48**, 11032–11044.
Luk, L. Y. P., Qian, Q. & Tanner, M. E. (2011). *J. Am. Chem. Soc.* **133**, 12342–12345.
Matthews, B. W. (1968). *J. Mol. Biol.* **33**, 491–497.
Metzger, U., Schall, C., Zocher, G., Unsöld, I., Stec, E., Li, S.-M., Heide, L. & Stehle, T. (2009). *Proc. Natl Acad. Sci. USA*, **106**, 14309–14314.
Otwinowski, Z. & Minor, W. (1997). *Methods Enzymol.* **276**, 307–326.
Steffan, N., Grundmann, A., Yin, W.-B., Kremer, A. & Li, S.-M. (2009). *Curr. Med. Chem.* **16**, 218–231.
Steffan, N., Unsöld, I. A. & Li, S.-M. (2007). *Chembiochem*, **8**, 1298–1307.
Unsöld, I. A. & Li, S.-M. (2005). *Microbiology*, **151**, 1499–1505.
Vagin, A. & Teplyakov, A. (2010). *Acta Cryst.* D**66**, 22–25.
Zou, H., Zheng, X. & Li, S.-M. (2009). *J. Nat. Prod.* **72**, 44–52.